Journal of Thermal Engineering, Vol. 4, No. 3, pp. 1984-1997, April, 2018
Yildiz Technical University Press, Istanbul, Turkey

THE NUMERICAL STUDY OF HEAT TRANSFER ENHANCEMENT USING AL_2O_3-WATER NANOFLUID IN CORRUGATED DUCT APPLICATION

N. Tokgoz[1,*], E. Alıç[2], Ö. Kaşka[3], M. M. Aksoy[4]

ABSTRACT

Heat transfer enhancement in channel flow is investigated in the present study by using corrugated duct in lieu of smooth duct. In this regard, periodic different cavities are applied on the duct walls using the same aspect ratios. The values of the Reynolds numbers are in the range of $10{,}000 \leq Re \leq 20{,}000$. The effects of the alumina-water nanofluid flow on the corrugated ducts are alternatively investigated by using the constant nanoparticle size for further improvement of the thermal characteristics. Computations are performed by means of finite volume approach on three different corrugated shapes. The effects of various parameters on the heat and fluid flow are also studied. The obtained results have revealed that the application of corrugated duct increases the rate of turbulent intensity on the central axis of the duct. In addition, it is found that the rate of heat transfer changes as a result of corrugated shape and Reynolds number. Furthermore, it is demonstrated that the application of the alumina-water flow in such ducts enhances the rate of the heat transfer and thermal performance when compared with the water flow. It is hoped that the obtained results will arouse interest towards thermal design.

Keywords: *Channel Flow, Corrugated Duct, Heat Transfer Enhancement, Nanofluid*

INTRODUCTION

Nanotechnology would be noted as the most important locomotive for the major industrial revolution of the present time. The poor performance of thermal conductivity of conventional fluids such as air, water, oil, and ethylene glycol mixture is the primary restriction to enhance the performance of heat exchangers [1]. Nanofluids are considered by suspending nanoparticles in conventional base liquids, and also the random motion process and dispersion structure of the suspended nanoparticles are the investigation fields of nanofluids [2]. Xuan and Li [3] have experimentally investigated the heat transfer and flow field of copper-water nanofluids flowing through a tube. They conclude their investment for a range of Re (10,000-25,000) and volume friction (0.3-2%). Yang et al [4] have investigated experimentally the convective heat transfer of graphite in oil nanofluid for laminar flow in a horizontal tube heat exchanger. Santra et al [5] showed that the heat transfer owing to laminar flow of copper-water nanofluid through two-dimensional channel with constant temperature walls and they conducted that the rate of heat transfer enhancement with the rising in flow Reynolds number, Re, as well as the increase in solid volume fraction. Kakac et al [6] revealed the nanofluid flow can be considered as a single-phase incompressible flow. Their investigation of the simplest approach for the single-phase assumption is the usage of the governing equations of pure fluid flow with taking the thermophysical properties of the nanofluid. Nield and Kuznetsov [7] made an analytical work of fully-developed laminar forced convection in a parallel-plate channel being concerned by a nanofluid which was subjected to uniform-flux boundary conditions, constant heat flux boundaries and constant temperature boundaries. Their model included the effects of Brownian motion and thermophoresis and they found that the combination of these effects caused decrease the Nusselt number. Selimefendigil and Oztop [8] implemented a numerical examination of laminar pulsating rectangular jet with nanofluids to investigate the effects of pulsating frequency, Reynolds number, and volume fraction on the nanofluid flow which can use heat transfer characteristics by using FLUENT finite volume-based code. From their results, in the pulsating flow case, the combined effect of pulsation and inclusion was not favorable for the rising of the stillness point. Manca et al [9] studied a numerical analysis on forced convection using Al_2O_3 nanoparticles in the water. They are considered the particle size is set equal to 38 nm, nanoparticle volume fractions from 0% to 4% and the flow regime is turbulent and Reynolds numbers are in the range 20,000-60,000.

This paper was recommended for publication in revised form by Regional Editor Ahmet Selim Dalkilic
[1]Department of Energy Systems Engineering, Osmaniye Korkut Ata University, Osmaniye, TURKEY
[2] Vocational School of Andırın, Sütçü İmam University,Kahramanmaraş, Turkey
[3] Department of Mechanical Engineering, Osmaniye Korkut Ata University, Osmaniye, TURKEY
[4] Department of Mechanical Engineering, Rice University, Houston, TX, USA
**E-mail address: nehirtokgoz@osmaniye.edu.tr*
Manuscript Received 9 August 2016, Accepted 14 September 2016

Their results indicate that particle volume concentration provides to proliferate heat transfer enhancement even though the minimum power to pump the nanofluid must be increased. Also, heat transfer coefficient and pressure loss are investigated by using artificial roughness ducts with grid ribs [10] and semi attached rib–groove channels [11]. Peng et al [12] stated that the 45° V-shaped continuous ribs among different V-shaped ribs have the best thermal achievement.

Promvonge et al [13] were carried a numerical analyze heat transfer characteristics in a square-duct with inline 60° V-shaped ribs placed on two opposite heated walls. It revealed the maximum thermal performance was around 1.8 for the rib with BR (rib height to duct diameter ratios) = 0.0725 where the heat transfer rate was about four times above the smooth duct at reduced Reynolds number. Choi [14] was the first who used the term nanofluids to refer to the fluids with suspended nanoparticles. Several researches have demonstrated that with low (1-5% by volume) nanoparticle concentrations, the thermal conductivity can be increased by about 20% [15-16]. Xuan et al [16] experimentally studied and obtained thermal conductivity of copper-water nanofluid up to 7.5% of solid volume fraction. Several researches have studied heat transfer enhancement with nanofluid [17-18]. Block and fin fitting in channel can be noted as control elements for rising or reducing of natural or forced convection heat transfer. Most of the investments on changing the flow pattern were performed using partitioning rectangular or square blockades [19-20]. Varol et al [21] studied the effects of fin placement on the bottom wall of a triangular enclosures filled with porous media.

Heidary et al [22] have researched free convection and entropy generation in an inclined square cavity filled with a porous medium. Valinataj-Bahnemiri et al [23] investigated of two-dimensional laminar flow of nanofluids in a sinusoidal wavy channel with uniform temperature grooved walls. Tiwari et al [24] studied the heat transfer effect and fluid flow characteristics of nanofluids CeO_2 and Al_2O_3 flowing in a counter flow. The corrugated plate heat exchanger has been simulated, and the three dimensional temperature graphs and velocity fields have been provided through computational fluid dynamics.

Darzi et al [25] experimentally studied to investigate the effect of nanoparticles on heat transfer and friction factor inside helically grooved tubes. Nanoparticles and helical grooves simultaneously augmented the heat transfers by factor of 3.2 for higher concentration of water-Al_2O_3 nanofluids. Navaei et al [26] investigated numerical simulations of turbulent forced convection heat transfer in a rib–groove duct exposed to uniform heat flux. Kareem et al [27] have researched spirally grooved tubes experimentally and numerically, they studied to analysis the effects of new spiral corrugation characteristics and showed the influence of the parameter called severity index on the total thermal performance. Ramadhan et al [28] investigated the fluid flow of turbulent heated flow inside a grooved tube and numerical analysis was used to find the heat transfers. Their study concerned fluid of air and grooved geometry for heat transfer enhancement.

To the best of our knowledge a few papers in the literature has so far studied heat transfer in different corrugated wall ducts with nanofluid. Therefore, the present study aims to extend the investigation of the effects of corrugated shape, nanoparticle and Reynolds number on heat transfer and flow behavior. Numerical method is employed for flow in channels having different corrugated shapes such as circular, triangular, and trapezoidal under constant wall temperatures with nanoparticle volume fraction 0.5% and Reynolds number ranging from 10,000 to 20,000.

MATERIAL AND METHOD

Problem Description and Numerical Method

In the present study, circular, triangular, and trapezoidal (namely Cr, Tr, and Trp, respectively) corrugated channels are investigated as can be seen in Figure 1, and it shows two-dimensional channels consist of different corrugated plates with amplitude of (h) and corrugation length of (e).

The width of the channel is very large compared to the height in order to shun from the effects of the side walls. All the cases have constant aspect ratio of h/D=0.2. The uniform temperature of the fluid at the inlet face is taken less than that of corrugated walls. The flow is taken Newtonian, two-dimensional and incompressible. The nanofluid which is modeled as a single-phase flow [29-30] is a mixture of water and uniform size and shape of solid spherical alumina particles. Nanoparticle size of 25 nm is used for water-alumina flow. The numerical simulations are performed over a range of Reynolds number, Re, $10{,}000 \leq Re \leq 20{,}000$ and nanoparticle volume concentration, φ, is 0.5. Non-conformal grid system is defined for each case.

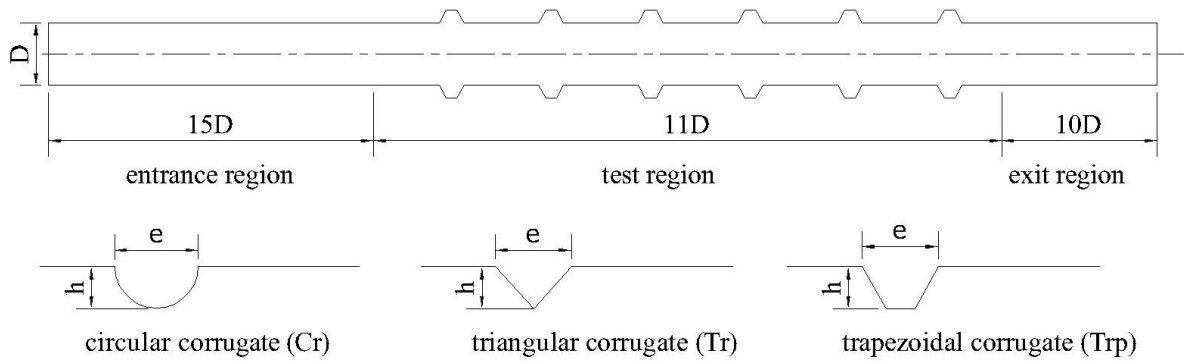

Figure 1. Schematic diagram of the corrugated channels studied

Computational fluid dynamics (CFD) package program FLUENT® was used to calculate the fluid flow and heat transfer in the present study. Standard k-ε method is conducted to analyze the turbulence characteristics, so that finite volume is being used to discretize the governing equations under steady state conditions. The standard k-ε model is widely used in industrial turbulent flow and heat transfer computations mainly due to its robustness, computational economy, and reasonable accuracy for a wide variety of turbulent flows. It is somewhat a semi empirical model, mainly because the modelled transport equation for dissipation used in the model depends on phenomenological considerations and empiricism. It is more expensive to implement than mixing length model or one equation model due to the use of two extra partial differential equations, as compared to zero- and one-equation transport equation, respectively, employed in the former models. In order to resolve the pressure-velocity system, SIMPLE algorithm [31] is used at this method, and also in computational domain, the convergence criteria was determined as 10^{-8} for all parameters.

Turbulence characteristics would be calculated by using the standard k-ε model. Utilization area of k-ε turbulence model is being criticized by some of the researchers [32] even though it has certainly been considered one of the modern methods for many researchers [33-35]. It can be considered that results of LES or DNS turbulence models can be evaluated satisfactory, yet computer workstation (i.e. ultrahigh-speed computer) should be needed.

Boundary Conditions and Governing Equations

Temperatures are kept constant at both lower and upper walls of the channels, and no slip condition is applied for the all wall surfaces. At the inlet, the flow has uniform temperature distribution. Fully developed flow is ensured before the test region. On the channel walls

$$u = v = w = 0 \qquad and \qquad T = T_w \tag{1}$$

On the channel axis

$$\frac{\partial \overline{u}}{\partial y} = \frac{\partial \overline{v}}{\partial y} = \frac{\partial \overline{w}}{\partial y} = \frac{\partial \overline{T}}{\partial y} \tag{2}$$

Calculations for a range of Reynolds number, $10{,}000 \leq Re \leq 20{,}000$ are performed from

$$\mathrm{Re} = \frac{\rho_f \overline{u} D_h}{\mu_f} \tag{3}$$

The continuity, momentum and energy equations can be seen below, respectively:

$$\frac{\partial}{\partial x_i}\left(\rho u_i\right) = 0 \tag{4}$$

$$\frac{\partial}{\partial x_i}\left(\rho u_i u_j\right) = -\frac{\partial p}{\partial x} + \frac{\partial}{\partial x_j}\left[\mu\left(\frac{\partial u_i}{\partial x_j} + \frac{\partial u_j}{\partial x_i}\right)\right] + \frac{\partial}{\partial x_j}\left(-\rho\overline{u_i' u_j'}\right) \tag{5}$$

$$\frac{\partial}{\partial x_i}\left(\rho u_i T\right) = \frac{\partial}{\partial x_j}\left[\left(\Gamma + \Gamma_t\right)\frac{\partial T}{\partial x_j}\right] \tag{6}$$

The molecular thermal diffusivity and turbulent thermal diffusivity are defined as

$$\Gamma = \frac{\mu}{\mathrm{Pr}} \quad \text{and} \quad \Gamma_t = \frac{\mu_t}{\mathrm{Pr}_t} \tag{7}$$

The last term of the momentum equation is called the Reynolds stresses. Boussinesq hypothesis can be used to model the Reynolds stresses in order to relate the Reynolds stresses to the mean velocity gradients. This relation is presented as

$$-\rho\overline{u_i' u_j'} = \mu_t\left(\frac{\partial u_i}{\partial x_j} + \frac{\partial u_j}{\partial x_i}\right) = \tau_{ij} \tag{8}$$

The turbulent or eddy viscosity with reference to applied turbulence model is

$$\mu_t = \rho C_\mu \frac{k^2}{\varepsilon} \tag{9}$$

The turbulent kinetic energy and the rate of turbulent kinetic energy dissipation are explained, respectively, as [33]:

$$\frac{\partial}{\partial x_i}\left(\rho k u_i\right) = \frac{\partial}{\partial x_j}\left[\left(\mu + \frac{\mu_t}{\sigma_k}\right)\frac{\partial k}{\partial x_j}\right] + G_k - \rho\varepsilon \tag{10}$$

$$\frac{\partial}{\partial x_i}\left(\rho\varepsilon u_i\right) = \frac{\partial}{\partial x_j}\left[\left(\mu + \frac{\mu_t}{\sigma_\varepsilon}\right)\frac{\partial \varepsilon}{\partial x_j}\right] + C_{\varepsilon 1}\frac{\varepsilon}{k}G_k - C_{\varepsilon 2}\rho\frac{\varepsilon^2}{k} \tag{11}$$

in which the rate of turbulent kinetic energy generation is [32]

$$G_k = -\rho\overline{u_i' u_j'}\frac{\partial u_j}{\partial x_i} \tag{12}$$

The closure coefficients are given by

$$C_{\varepsilon 1} = 1.44, \quad C_{\varepsilon 2} = 1.92, \quad C_\mu = 0.09, \quad \sigma_k = 1.0$$

The density, heat capacity, thermal conductivity and viscosity values of nanofluid obtained from Sahin [36]. Details of properties of nanofluid are given in Table 1.

Table 1. Thermophysical properties of Al_2O_3 [23]

Volume concentration, φ (%)	Thermal conductivity k_{nf} (W/mK)	Density ρ_{nf}, (kg/m^3)	Heat capacity C_{Pnf} (J/kgK)	Viscocity μ_{nf} (kg/ms)
0.5	0.62178	1010.82	4114.61	0.0008797

Using the following equation, the surface heat transfer coefficient is estimated.

$$h(x) = \frac{q''(x)}{T_w - T_m} \tag{13}$$

where T_m, is bulk temperature which can be determined as [23]

$$T_m = \frac{\int_0^{H/2} uTdA}{\int_0^{H/2} udA} \tag{14}$$

Also, the value of the local Nusselt number is computed using the following correlation

$$Nu = \frac{hD_h}{k} \tag{15}$$

Furthermore, the value of the mean Nusselt number is obtained by integration of Eq. (16) over the corrugated duct surface as

$$\overline{Nu} = \frac{1}{\xi}\int_0^{\xi} Nudx \tag{16}$$

where

$$\xi = \sum_{i=0}^{i=n}(p_i + S_i) \tag{17}$$

The friction factor is calculated from

$$\mathrm{f} = \Delta \mathrm{p}\frac{2\mathrm{D_h}}{\mathrm{L}\left(\rho \mathrm{u}^{-2}\right)} \tag{18}$$

The thermal performance, η is calculated from

$$\eta = \frac{\overline{\frac{Nu}{Nu_s}}}{\left(\frac{f}{f_s}\right)^{1/3}} \tag{19}$$

η, the thermal performance relates the heat transfer enhancement (Nu/Nu_s, ratio of Nusselt number in the corrugated channel in comparison to that in the smooth channel) and pressure drop increase (f/fs), ratio of friction factor in the corrugated channel in comparison to that in the smooth channel), where in the dimensionless quantity of a rough surface is referred to that of a smooth surface. In the interest of heat transfer enhancement, the thermal performance must be greater than 1.

Validation of Numerical Study

To validate the numerical predictions, the thermal-hydraulic characteristics are computed for plain duct using different Reynolds numbers and are compared with well-known correlation. Pethukov [37] correlation defined as Eq. (20) and Blasius correlation defined as Eq. (21) are used for friction comparison through pure water flow in smooth channel. The Nusselt number obtained from the smooth duct were compared with Dittus-Boelter and Pethukov correlations defined as Eq. (22), Eq. (23) respectively. In addition to this validation, the present numerical results are compared with the obtained from Sahin's experimental study for nanofluid (5%) flow.

$$f = (0.790 \ln \mathrm{Re}_d - 1.64)^{-2} \tag{20}$$

$$f = 0.316(\mathrm{Re}_D)^{-0.25} \tag{21}$$

$$Nu = 0.023 \mathrm{Re}^{0.8} \mathrm{Pr}^{0.4} \tag{22}$$

$$Nu = \frac{\left(\frac{f}{8}\right)\mathrm{Re}\,\mathrm{Pr}}{1.07 + 12.7\left(\frac{f}{8}\right)^{0.5}(\mathrm{Pr}^{0.67} - 1)} \tag{23}$$

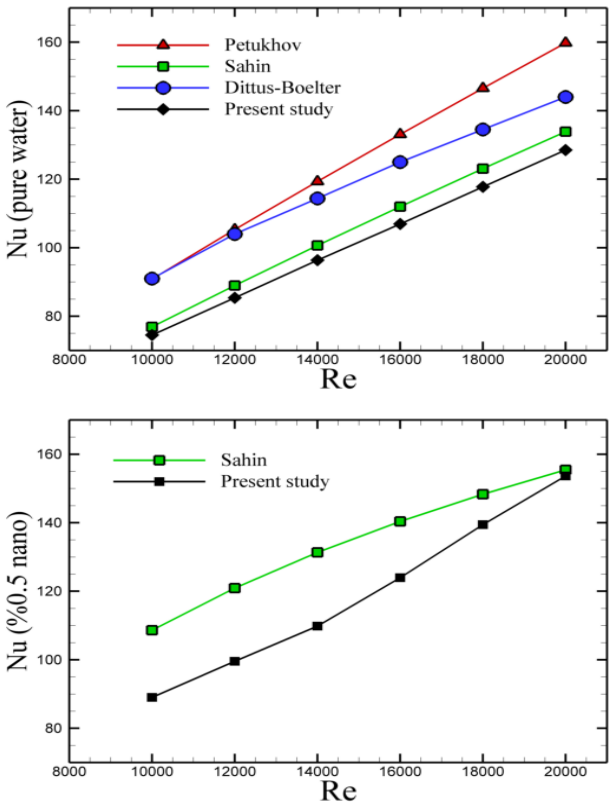

Figure 2. Comparison of the Nusselt number with the well-known correlations for pure water and nanofluid

Figure 2 and 3 demonstrates the variations over Nusselt number and the friction factor as functions of the Reynolds number. It is observed that the predicted thermal-hydraulic characteristics match with previous analytics and experimental results for pure water. Furthermore, the present numerical results reasonably agree well within 13% deviation for nanofluid Nusselt number predictions.

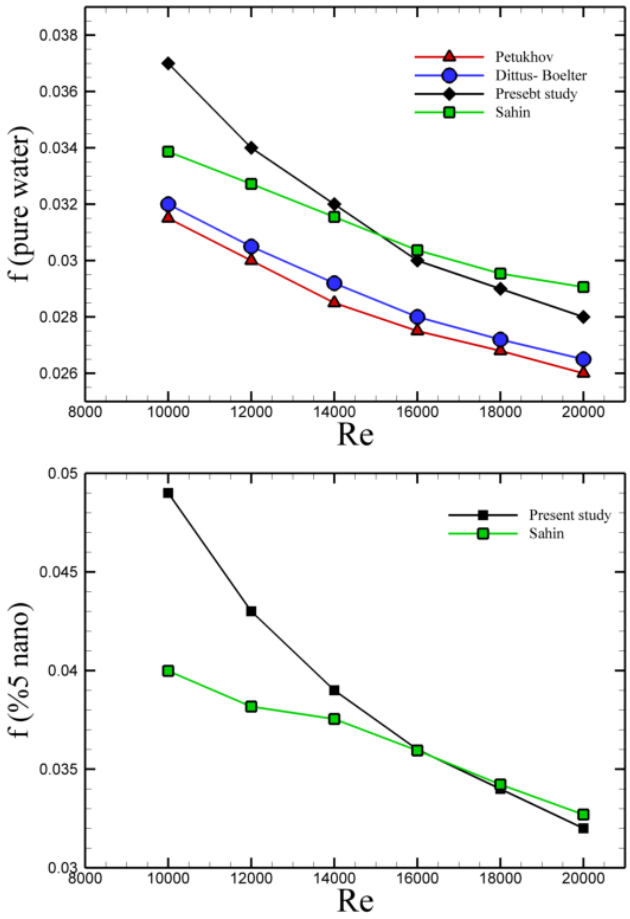

Figure 3. Comparison of the friction factor with the well-known correlations for pure water and nanofluid

Grid Size Independence Study

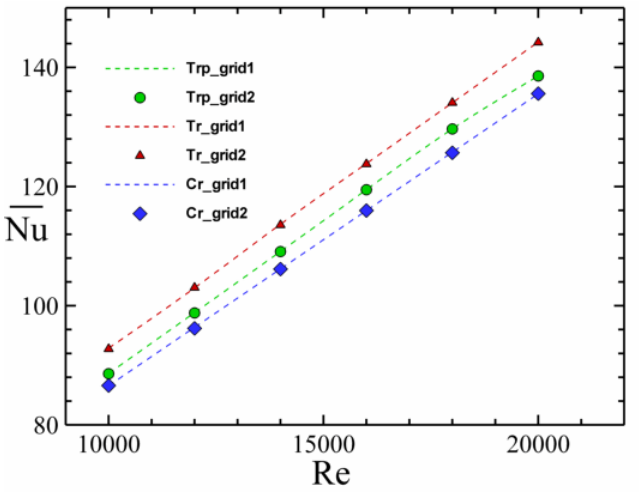

Figure 4. Grid size independence study results

In order to study the grid size (mesh) independence of the results, two different grid sizes are scrutinized for triangular (Tr), trapezoidal (Trp) and circular (Cr) corrugated channels. The first grid system (present grid system) has the minimum element size of λ/H=0.0005 and the finer grid system has the minimum element size of λ/H=0.0004 near the corrugated duct walls. In this regard, Figure 4 shows the grid size independence results for water flow in all three-corrugated duct. As can be seen, the values of the friction factor and mean Nusselt number are not altered using the finer element size.

RESULTS AND DISCUSSION

Geometry Effects

In order to see the effects of corrugated shape on the thermal-hydraulic characteristics, water flow in four geometries are studied and obtained results are compared with that of smooth duct. Figure 5 reveals the friction factor variations for different Reynolds numbers. The first row of Figure 5 shows the effects of corrugated shape on the variation of the average Nusselt with Reynolds number. Since the flow mixing increases with using plate corrugations, the rate of heat transfer and the thermal efficiency for all cases are higher than those of the smooth duct. The Nusselt number increases with Reynolds number as expected. The enhancement on the heat transfer is proportional to the corrugation channel and the Reynolds number as shown in second row of Figure 5.

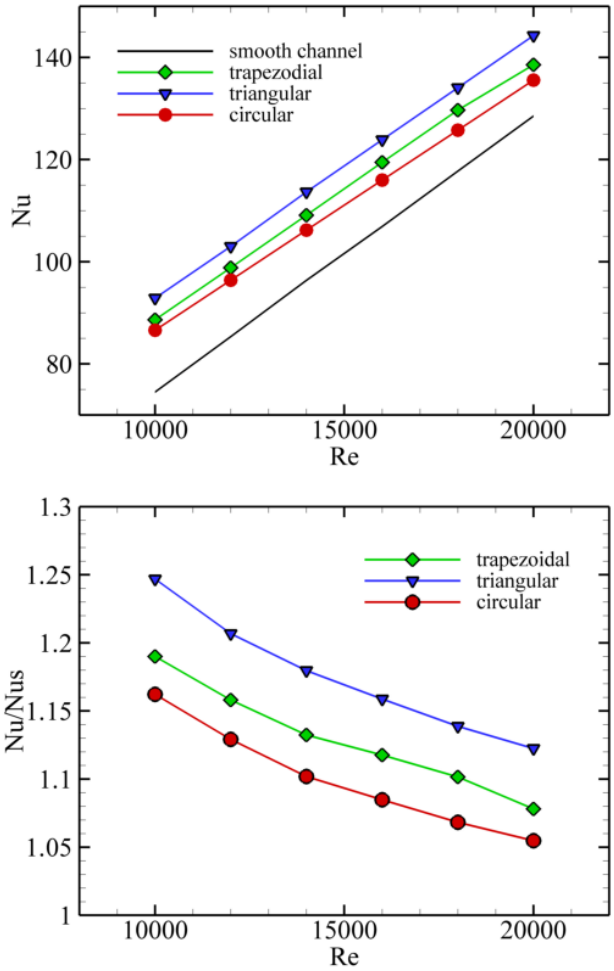

Figure 5. Variation of the Nusselt number, Nu with the Reynolds number, Re for all cases with smooth channel data

In generally, as fluid flow through the corrugated surface, the fluid recirculation flows are generated in the corrugation troughs. The onset and growth of recirculation zones promote the mixing of fluid in the boundary layer and as a result, the heat transfer enhancement is observed. Therefore, ratio of Nu in the corrugated channel to that in the straight channel (Nu/Nu_s) is adopted in order to reveal the heat transfer enhancement as to compare

the performance between corrugated channels and straight channel. From the second row of Figure 5, it can be inferred that the effect of corrugations on heat transfer rate is more efficient at a lower Reynolds number. This situation can be related to the thickness of the thermal boundary layer because the thermal boundary layer becomes thicker at the lower Reynolds number and so, the outcome of the disruption of the thermal boundary layer becomes more appreciable. For studied aspect ratio (h/D=0.2), the highest values of Nusselt number obtained by triangular, trapezoidal and circular corrugated duct, respectively. The triangular shape indicates the highest value for enhancing Nusselt number as it has the most significant role in the pulling up and down of the thermal boundary layer periodically. That is, the fluid filling the groove surface will be pulsed through the sweeping along the test section. Figure 6 reveals the friction factor variations for different Reynolds numbers and volume fraction of the nanoparticle is 5%.

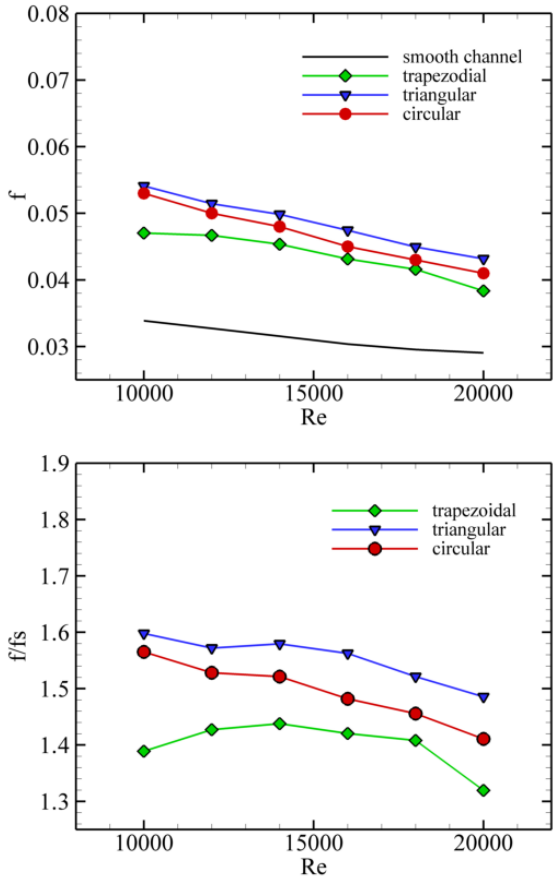

Figure 6. Variation of friction factor, *f* with the Reynolds number, Re for all comparison with smooth channel data

Development of the turbulent flow in the corrugated channels influences the friction factor, *f* as a main hydraulic characteristic of the flow. The friction factor, *f* in comparison to that of the straight channel surface is clearly presented in Figure 6. It is obvious that the friction factor decreases gradually for all configurations as a result of the increase of Reynolds number, *Re*. From the mean values of the friction factor, the lower one is hit by the trapezoidal duct for full range of Reynolds numbers while the next steps are taken by circular and triangular. Logical explanation of this result would be that active flow recirculation region is being occurred at sharp edges of the trapezoidal region due to far distance among these edges even though total area of trapezoidal area is higher than triangular area, and finally it causes the possibility of showing low resistance to the flow compared to the others. Enlarging the area of this recirculation, especially for rectangular groove, it causes to drag the fully developed fluid flow, and therefore these vortices induce to increase in the friction coefficient as well as the required pumping pressure.

Nanofluid Effects

Heat transfer and flow behavior of nanofluid flow in channel with rectangular corrugations for corrugated shape and Reynolds numbers are illustrated and obtained results are compared with those of water flow.

The variation of the Nusselt number for corrugated channel with the Reynolds numbers is presented in Figure 7. By using either nanofluid or pure water, the Nusselt number increases with the increase of the Reynolds number. It can be deduced that addition of nanoparticles into pure water augments heat transfer in cases where the particle volume concentrations are found to be lower than 1 vol. % such as 0.5% [36]. Nevertheless, the Nusselt number for nanofluid is higher than that of pure water within the range of 10% to 15%. The highest enhancements in Nusselt number are found at Reynolds number of 10,000 at triangular corrugated channel with the enhancement of 15% compared the water.

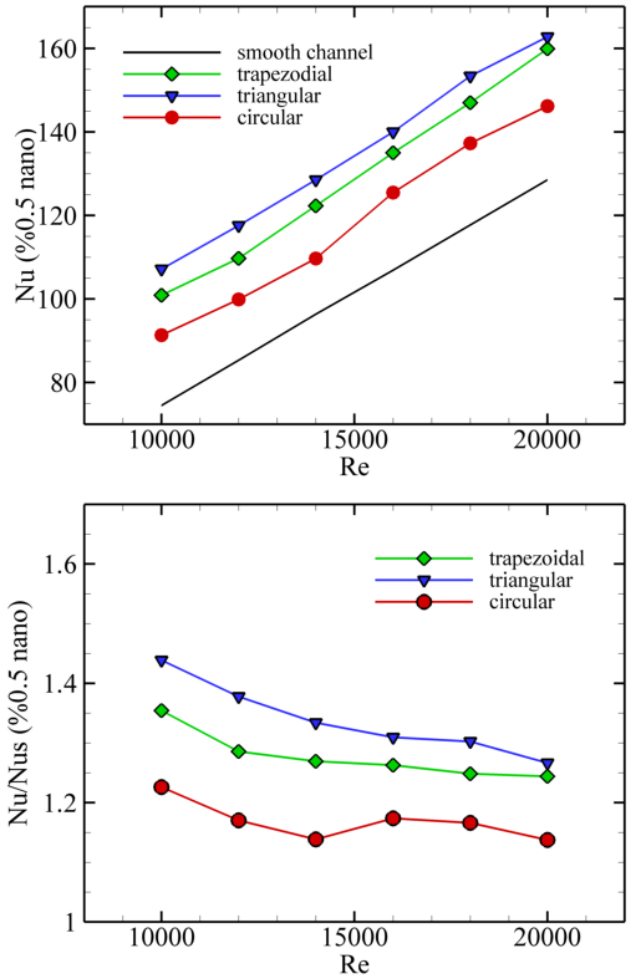

Figure 7. Effect of nanoparticle on Nusselt number for corrugated channel.

As the use of nanofluids in corrugated channels raises both Nusselt number and friction factor, thermal performance, η (which depends upon friction factor, f and Nusselt number), of flow should be calculated in order to find the optimum case. Figure 8 indicates the thermal performance variation with Reynolds number for different corrugated channels.

It is seen that thermal performance decreases slightly with Reynolds number. Among all cases, thermal performance of triangular corrugated has highest value. Because of friction factor, the trend of the thermal performance is not similar to one another. Simple physics suggests that enhancing the rate of heat transfer slightly is possible. Nevertheless, other problems such as segregations arise while adding nanoparticles, and agglomeration should be taken into consideration in the practical application. However, the addition of

nanoparticles into light fluids (compared with the density of fluid) reduces buoyancy force and decreases the natural convection rate of heat transfer [38].

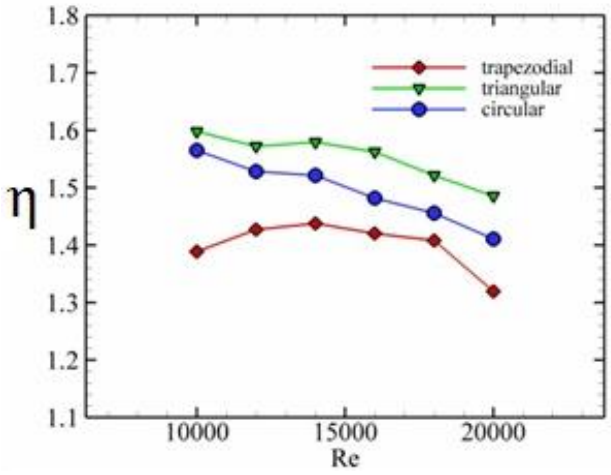

Figure 8. Variations of thermal performance with the Reynolds number for all geometric configurations

CONCLUSION

In the present study, heat transfer enhancement and flow characteristics of alumina-water nanofluid through corrugated channel with different geometric shapes are numerically investigated for a Reynolds number range of 10,000-20,000 and nanoparticle volume fraction is taken as 0.5%. The finite volume method is used in order to solve the governing equations numerically. Three main goals are illustrated in this study which they are the effects of nanoparticle, corrugated shape and Reynolds number on flow behavior, and heat transfer rate. Turbulence flow is created as a result of the corrugations because it provides to increase flow mixing and heat transfer enhancement. The turbulence intensity rate increases with Reynolds number. However, it is observed that heat transfer between the walls and the fluid can considerably increase with addition of nanoparticles to the water. On the other hand, using alumina-water nanofluid flow gives rise to additional enhancements on the rate of heat transfer. The results of the present study reveal that using nanofluids instead of conventional fluids would lead to further improvement in thermal performance of heat exchangers for appropriate Reynolds number regime. Moreover, the addition of such particles has the possibility of increasing the effective viscosity of a flow, which affects the forced convection and pressure drop adversely. Besides, the erosion may be enhanced because of impingement of those particles on the surfaces. Additionally, the use of already established correlation for the rate of heat transfer can be extended to the nanofluid without further investigation into the impact of nanofluids on the convective heat transfer [33].

NOMENCLATURE

c_p	Specific heat (J/kgK)
C_μ	Turbulence model constant
D_h	Hydraulic diameter, D, (m)
F	Friction factor
h	Heat transfer coefficient (W/m^2 K)
k	Turbulent kinetic energy
k_f	Thermal conductivity of fluid (W/mK)
Nu	Nusselt number
Pr	Prandtl number
Re	Reynolds number
T	Temperature (K)
U	Mean velocity (m/s)
X	Axial coordinate
Y	Vertical coordinate

Γ	Thermal diffusivity (m^2/s)
E	Turbulent dissipation rate (m^2/s^3)
H	(-)
μ	Viscosity (kg/ms)
μ_t	Eddy viscosity (kg/m s)
ρ	Density (kg/m^3)
τ_{ij}	Reynolds stress, (m^2/s^2)
φ	Volume concentration (%)
f	Fluid
i	Inlet
m	Mean
nf	Nanofluid
s	Smooth
t	Turbulent
w	Wall

REFERENCES

[1] Khanafer, K., Vafai, K., & Lightstone, M. (2003). Buoyancy-driven heat transfer enhancement in a two-dimensional enclosure utilizing nanofluids. International Journal of Heat and Mass Transfer, 46(19), 3639-3653.

[2] Xuan, Y., Li, Q., & Hu, W. (2003). Aggregation structure and thermal conductivity of nanofluids. AIChE Journal, 49(4), 1038-1043.

[3] Xuan, Y., & Li, Q. (2003). Investigation on convective heat transfer and flow features of nanofluids. Journal of Heat transfer, 125(1), 151-155.

[4] Yang, Y., Zhang, Z. G., Grulke, E. A., Anderson, W. B., & Wu, G. (2005). Heat transfer properties of nanoparticle-in-fluid dispersions (nanofluids) in laminar flow. International Journal of Heat and Mass Transfer, 48(6), 1107-1116.

[5] Santra, A. K., Sen, S., & Chakraborty, N. (2009). Study of heat transfer due to laminar flow of copper–water nanofluid through two isothermally heated parallel plates. International Journal of Thermal Sciences, 48(2), 391-400.

[6] Kakaç, S., & Pramuanjaroenkij, A. (2009). Review of convective heat transfer enhancement with nanofluids. International Journal of Heat and Mass Transfer, 52(13-14), 3187-3196.

[7] Nield, D., & Kuznetsov, A. (2014). Forced convection in a parallel-plate channel occupied by a nanofluid or a porous medium saturated by a nanofluid. International Journal of Heat and Mass Transfer, 70, 430-433.

[8] Selimefendigil, F., & Öztop, H. F. (2014). Pulsating nanofluids jet impingement cooling of a heated horizontal surface. International Journal of Heat and Mass Transfer, 69, 54-65.

[9] Manca, O., Nardini, S., & Ricci, D. (2012). A numerical study of nanofluid forced convection in ribbed channels. Applied Thermal Engineering, 37, 280-292.

[10] Karmare, S., & Tikekar, A. (2007). Heat transfer and friction factor correlation for artificially roughened duct with metal grit ribs. International Journal of Heat and Mass Transfer, 50(21-22), 4342-4351.

[11] Liu, H., & Wang, J. (2011). Numerical investigation on synthetical performances of fluid flow and heat transfer of semiattached rib-channels. International Journal of Heat and Mass Transfer, 54(1-3), 575-583.

[12] Peng, W., Jiang, P.-X., Wang, Y.-P., & Wei, B.-Y. (2011). Experimental and numerical investigation of convection heat transfer in channels with different types of ribs. Applied Thermal Engineering, 31(14-15), 2702-2708.

[13] Promvonge, P., Changcharoen, W., Kwankaomeng, S., & Thianpong, C. (2011). Numerical heat transfer study of turbulent square-duct flow through inline V-shaped discrete ribs. International Communications in Heat and Mass Transfer, 38(10), 1392-1399.

[14] Choi, S. U., & Eastman, J. A. (1995). Enhancing thermal conductivity of fluids with nanoparticles. (No. ANL/MSD/CP--84938; CONF-951135--29). Argonne National Lab., IL (United States).

[15] Lee, S., Choi, S. S., Li, S. A., and, & Eastman, J. A. (1999). Measuring thermal conductivity of fluids containing oxide nanoparticles. Journal of Heat transfer, 121(2), 280-289.

[16] Xuan, Y., & Li, Q. (2000). Heat transfer enhancement of nanofluids. International Journal of heat and fluid flow, 21(1), 58-64.
[17] Das, S. K., Choi, S. U., Yu, W., & Pradeep, T. (2007). Nanofluids: science and technology: John Wiley & Sons.
[18] Ding, Y., Chen, H., Wang, L., Yang, C. Y., He, Y., Yang, W., … & Huo, R. (2007). Heat transfer intensification using nanofluids. KONA Powder and Particle Journal, 25, 23-38.
[19] Bilgen, E. (2005). Natural convection in cavities with a thin fin on the hot wall. International Journal of Heat and Mass Transfer, 48(17), 3493-3505.
[20] Hasnaoui, M., Bilgen, E., & Vasseur, P. (1991). Natural convection above an array of open cavities heated from below. Numerical Heat Transfer, 18(4), 463-482.
[21] Varol, Y., Oztop, H. F., & Varol, A. (2007). Natural convection in porous triangular enclosures with a solid adiabatic fin attached to the horizontal wall. International Communications in Heat and Mass Transfer, 34(1), 19-27.
[22] Heidary, H., Pirmohammadi, M., & Davoudi, M. (2012). Control of free convection and entropy generation in inclined porous media. Heat Transfer Engineering, 33(6), 565-573.
[23] Valinataj-Bahnemiri, P., Ramiar, A., Manavi, S., & Mozaffari, A. (2015). Heat transfer optimization of two phase modeling of nanofluid in a sinusoidal wavy channel using Artificial Bee Colony technique. Engineering Science and Technology, an International Journal, 18(4), 727-737.
[24] Tiwari, A. K., Ghosh, P., Sarkar, J., Dahiya, H., & Parekh, J. (2014). Numerical investigation of heat transfer and fluid flow in plate heat exchanger using nanofluids. International Journal of Thermal Sciences, 85, 93-103.
[25] Darzi, A. A. R., Farhadi, M., & Sedighi, K. (2014). Experimental investigation of convective heat transfer and friction factor of Al2O3/water nanofluid in helically corrugated tube. Experimental Thermal and Fluid Science, 57, 188-199.
[26] Navaei, A., Mohammed, H., Munisamy, K., Yarmand, H., & Gharehkhani, S. (2015). Heat transfer enhancement of turbulent nanofluid flow over various types of internally corrugated channels. Powder Technology, 286, 332-341.
[27] Kareem, Z. S., Abdullah, S., Lazim, T. M., Jaafar, M. M., & Wahid, A. F. A. (2015). Heat transfer enhancement in three-start spirally corrugated tube: Experimental and numerical study. Chemical Engineering Science, 134, 746-757.
[28] Ramadhan, A. A., Al Anii, Y. T., & Shareef, A. J. (2013). Groove geometry effects on turbulent heat transfer and fluid flow. Heat and Mass Transfer, 49(2), 185-195
[29] Sharma, K., Sundar, L. S., & Sarma, P. (2009). Estimation of heat transfer coefficient and friction factor in the transition flow with low volume concentration of Al2O3 nanofluid flowing in a circular tube and with twisted tape insert. International Communications in Heat and Mass Transfer, 36(5), 503-507.
[30] Shahi, M., Mahmoudi, A. H., & Talebi, F. (2011). A numerical investigation of conjugated-natural convection heat transfer enhancement of a nanofluid in an annular tube driven by inner heat generating solid cylinder. International Communications in Heat and Mass Transfer, 38(4), 533-542.
[31] Patankar, S. (1980). Numerical heat transfer and fluid flow. CRC press.
[32] Wilcox, D. C. (1988). Reassessment of the scale-determining equation for advanced turbulence models. AIAA journal, 26(11), 1299-1310.
[33] Vanaki, S. M., Mohammed, H., Abdollahi, A., & Wahid, M. (2014). Effect of nanoparticle shapes on the heat transfer enhancement in a wavy channel with different phase shifts. Journal of Molecular Liquids, 196, 32-42.
[34] Weihing, P., Younis, B., & Weigand, B. (2014). Heat transfer enhancement in a ribbed channel: Development of turbulence closures. International Journal of Heat and Mass Transfer, 76, 509-522.
[35] Ağra, Ö., Demir, H., Atayılmaz, Ş. Ö., Kantaş, F., & Dalkılıç, A. S. (2011). Numerical investigation of heat transfer and pressure drop in enhanced tubes. International Communications in Heat and Mass Transfer, 38(10), 1384-1391.
[36] Sahin, B., Gültekin, G. G., Manay, E., & Karagoz, S. (2013). Experimental investigation of heat transfer and pressure drop characteristics of Al2O3–water nanofluid. Experimental Thermal and Fluid Science, 50, 21-28.
[37] Petukhov, B. (1970). Heat transfer and friction in turbulent pipe flow with variable physical properties Advances in heat transfer (Vol. 6, pp. 503-564): Elsevier.

[38] Mohamad, A. (2015). Myth about nano-fluid heat transfer enhancement. International Journal of Heat and Mass Transfer, 86, 397-403.